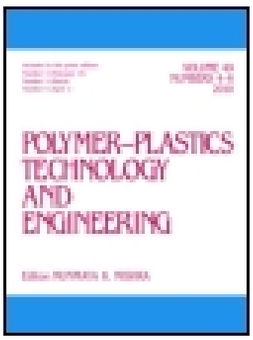

Polymer-Plastics Technology and Engineering

ISSN: 0360-2559 (Print) 1525-6111 (Online) Journal homepage: http://www.tandfonline.com/loi/lpte20

Development and Study of Solid Polymer Electrolyte Based on Polyvinyl Alcohol: $Mg(ClO_4)_2$

Mangalam Ramaswamy, Thamilselvan Malayandi, Selvasekarapandian Subramanian, Jayakumar Srinivasalu, Manjuladevi Rangaswamy & Vairam Soundararajan

To cite this article: Mangalam Ramaswamy, Thamilselvan Malayandi, Selvasekarapandian Subramanian, Jayakumar Srinivasalu, Manjuladevi Rangaswamy & Vairam Soundararajan (2017): Development and Study of Solid Polymer Electrolyte Based on Polyvinyl Alcohol: $Mg(ClO_4)_2$, Polymer-Plastics Technology and Engineering, DOI: 10.1080/03602559.2016.1247280

To link to this article: http://dx.doi.org/10.1080/03602559.2016.1247280

Accepted author version posted online: 10 Mar 2017.

Development and Study of Solid Polymer Electrolyte Based on Polyvinyl Alcohol : $Mg(ClO_4)_2$

Mangalam Ramaswamy[1], Thamilselvan Malayandi[2], Selvasekarapandian Subramanian[3], Jayakumar Srinivasalu[1], Manjuladevi Rangaswamy[4], Vairam Soundararajan[5]

[1]Department of Physics, PSG Institute of Technology and Applied Research, Coimbatore Tamilnadu, India
[2]Department of Physics, Thanthai Periyar Government Institute of Technology, Vellore, Tamilnadu, India
[3]Materials Research Center, Coimbatore, India
[4]Department of Physics, SriGuru Institute of Technology, Coimbatore, Tamilnadu, India
[5]Department of Chemistry, Government College of Technology, Coimbatore, Tamilnadu, India

Corresponding to author: Selvasekarapandian Subramanian, E-mail: sekarapandian@rediffmail.com

Abstract

Magnesium ion conducting solid polymer electrolytes (SPE) consisting of polyvinyl alcohol (PVA) with magnesium perchlorate ($Mg(ClO_4)_2$) as electrolytic salt have been developed and their experimental investigations are reported. The SPEs have been prepared by well known solution casting method using double distilled water as solvent. The highest room temperature conductivity of the order of 10^{-4} S/cm was obtained for the SPE with the composition 80 mol% PVA: 20 mol% $Mg(ClO_4)_2$. The pattern of the temperature-dependent conductivity shows Arrhenius behaviour. The FTIR analysis confirms the complex formation of the polymer with the salt. The XRD results reveal that the crystalline phase of polymer host has completely changed on the addition of dopant. DSC studies show a decrease in melting temperature of the PVA with increasing dopant concentration. The real part of dielectric permittivity shows a strong dispersion at lower frequencies, which implies the space charge effects arising from the electrodes. The loss tangent spectrum reveals that the jumping probability per unit time decreases with increasing salt concentration. The total ionic transference number measured has been

found to be in the range of 0.92–0.94 for all the polymer electrolyte systems. The result reveals that the conducting species are predominantly ions. The SPE with highest conductivity showed an electrochemical stability of 2 V. Results obtained by cyclic voltammetry on SS/SPE/SS, Mg/SPE/Mg symmetrical cells show evidence for reversibility.

Graphical Abstract

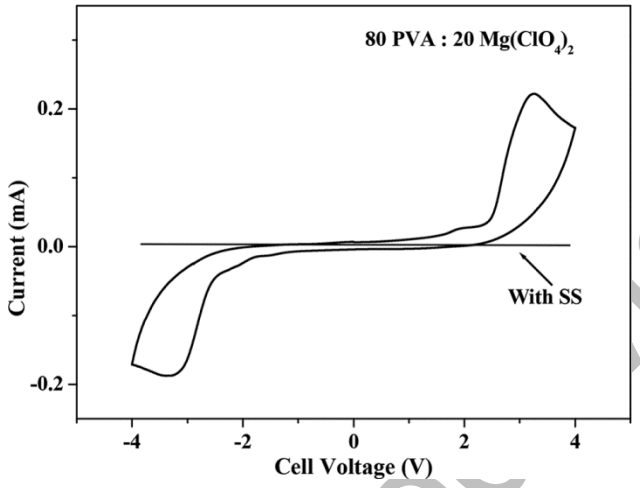

KEYWORDS: Polyvinyl alcohol, Mg ion, XRD, FTIR, ac impedance, cyclic voltammetry

1. INTRODUCTION

Rechargeable magnesium batteries have attracted increasing attention over the past few years in view of negligible hazards and enhanced safety. Magnesium is more stable than both lithium or sodium and it can be handled safely in open air. In spite of its natural abundance, low equivalent weight (12 g/F, as compared to 7 g/F for Li or 23 g/F for Na), significantly higher volumetric capacity (i.e., 3832 mAh cm^{-3}_{Mg}, 2062 mAh cm^{-3}_{Li} and 1136 mAh cm^{-3}_{Na}) and inexpensive, the development of Mg batteries has been hampered

by a variety of intrinsic problems related to i) the sluggish Mg intercalation and deintercalation in cathode materials ii) lack of appropriate nonaqueous media that conduct Mg^{2+} ions [1-7]. However, passivation free situation for Mg electrodes exists indeed in Grignard solutions (RMgX in ethers, R = organic alkyl or aryl group and X = halide like Cl^- or Br^-). Yet the commercialization of those batteries using Grignard reagents was not successful in view of i) low anodic stability, ii) too narrow voltage window and iii) low ionic conductivity. Thus an ideal electrolyte system with sufficiently high ionic conductivity, wider electrochemical stability and non-flammable is highly desirable for ultimate industrialization of Mg secondary batteries [8,9].

A mechanically robust membrane with high ionic conductivity at room temperature is the important criterion for its practical application in all electrochemical devices. Literature provides details of polymeric solid electrolytes based on PEO (polyethylene oxide) with Mg salts [10-14]. The conductivity of the most widely studied PEO electrolytes was typically 10^{-5} S/cm or lower at room temperature. Recently, many Mg^{2+} ion conducting gel polymer electrolytes are also reported which are useful for Mg-batteries and other electrochemical applications [15- 18]. Among the polymers reported in literature, polyvinyl alcohol (PVA) can be leveraged as a polymer matrix because of its good film forming capacity, better electrochemical stability, good mechanical properties and non-toxic in nature [19-21]. It has carbon chain backbone with hydroxyl groups attached to methane carbons (CH_2 - CH) which can be a source of hydrogen bonding and hence, assist the formation of polymer electrolytes. A R Polu et al. have obtained an ionic conductivity of 10^{-7} S/cm at RT in PVA based polymer electrolytes with $Mg(CH_3COO)_2$

and $Mg(NO_3)_2$ as dopant salts [22,23]. In the present paper, the electrochemical properties of PVA based Mg^{2+} ion conducting polymer electrolyte complexed with magnesium perchlorate ($Mg(ClO_4)_2$) are investigated for its application in the rechargeable magnesium batteries. The electrolytes have been characterized using various experimental techniques, namely Fourier transform infrared spectroscopy (FTIR), X-ray Diffraction (XRD), Differential scanning calorimetry (DSC), complex impedance analysis, linear sweep voltammetry (LSV) and cyclic voltammetry (CV).

2. EXPERIMENTAL

Sample Preparation

PVA (88% hydrolysed) with an average molecular weight (1,25,000, Sd Fine) and magnesium perchlorate ($Mg(ClO_4)_2$, Merck) were used as the raw materials in the present study. A solution casting method was used to prepare the polymer electrolytes with double distilled water as the solvent. Polymer electrolytes of various compositions have been prepared by varying the polymer and salt concentrations in the mole ratio (Table. 1). Right quantity of PVA was dissolved in doubled distilled water with continuous stirring at 50^{o}C for 6 hours. After the complete dissolution of the polymer in the solvent, required amount of $Mg(ClO_4)_2$ was added and the mixture was continuously stirred for about 12 hours at room temperature to obtain a clear homogeneous solution. The obtained solution was then casted on polypropylene petridishes and allowed to dry at room temperature for 7 days. Utmost care was taken to remove the residual traces of the water molecules by drying the films in air oven at 80^{o}C for 72 hr and then at 80^{o}C for 48 hr in vacuum oven. It is well known that even a small amount of moisture would raise dramatically the

conductivity of the samples; the films were stored in vacuum desiccators until further use to avoid moisture absorption. The obtained polymer electrolyte films were flexible, transparent and free standing.

Sample Characterization

In order to investigate the crystallinity of the polymer electrolytes, X – ray diffraction scans were taken in the range of 10^{o} to 80^{o} using Philips X'Pert PRO diffractometer at room temperature. The polymer electrolytes were subjected to FTIR study to investigate the complexation using Shimadzu 8000 spectrophotometer in the wave number ranging 400 – 4000cm^{-1}. The melting temperature of the solid polymer electrolytes was obtained from DSC measurements using a MAS-5800 model DSC 200 differential scanning calorimeter in N_2 atmosphere with a heating rate of 10°C/min. The electrical conductivity of the polymer electrolytes was measured using a HIOKI 3532 LCR impedance analyzer interfaced with a computer in the frequency range of 42 Hz – 5 MHz in the temperature range of 303 – 353 K using stainless steel (SS) as the blocking electrodes. The electrochemical properties of the symmetrical cells were recorded using potentiostat/galvanostat (EG&G PARC Model Versastat).

3. RESULTS AND DISCUSSION

3.1. XRD Analysis

Fig. 1 shows the XRD pattern of $Mg(ClO_4)_2$, pure PVA and PVA doped with different mole ratios of $Mg(ClO_4)_2$. The XRD pattern of pure PVA (Fig. 1) exhibits a peak at 2θ = 19.9 ^{o} corresponding to the (110) reflection [23]. The XRD patterns of PVA doped with different mole ratio of $Mg(ClO_4)_2$ show a gradual increase in the width and decrease in

the intensity of the peak at 19.9^{o} with an increase in the concentration of $Mg(ClO_4)_2$. The reduction in the intensity of the peak and the gradual increase in the width of the peak is a clear indication of the increase in the degree of amorphous nature. Due to the blending of dopant with PVA, the cation of the dopant is likely to interact with the hydroxyl group of PVA whereas, the anions are weakly coordinated and are stabilized by close association with the cations, which is believed to function as a plasticizer [24]. The peaks corresponding to $Mg(ClO_4)_2$ were found to be absent in the polymer complexes. Similar results have been reported for PEO- $Mg(ClO_4)_2$ polymer electrolytes [25]. 80 PVA : 20 $Mg(ClO_4)_2$ polymer membrane is more amorphous in nature compared to other polymer membranes. The amorphous nature of the polymer membrane can be interpreted in terms of Hodge et al. [26] criterion, which has established a correlation between the height of the peak and degree of crystallinity. The crystallites size for electrolytes shown in the figure have been calculated by Debye-Scherrer's equation,

$$D = \frac{0.89}{\beta cos\theta} \qquad (1)$$

where λ, is the wavelength of x- ray radiation, β is the full width of half maximum and θ is the diffraction angle. The intensity of the peak (height) and full width half maximum (β) corresponding to 2θ are calculated by fitting the peak with guassian fit. Table :1 shows the crystallite size of the samples.

3.2. FTIR Analysis

FTIR spectroscopy is used to establish interaction(s) between the polymer (PVA) and the dopant $Mg(ClO_4)_2$. Such interactions can induce changes in the vibrational modes of the atom or molecule in the material. Fig. 2 shows the infrared spectra and assignment of the

most evident absorption bands for pure PVA and polymer electrolytes doped with different mole ratios of $Mg(ClO_4)_2$ between 400 and 4000 cm^{-1}. The band assignments of the polymer electrolytes are given in Table. 2. A broad peak centred around 3307 cm^{-1} is assigned to the stretching vibration of the hydroxyl group (O – H) of pure PVA [27]. The shifting and broadening of this peak (3340 – 3392) in the polymer complexes indicates the coordination between the cation of the dopant and the hydroxyl group of PVA [28]. Mg^{2+} is an electrophile which seeks electron rich atom to interact and possibly makes an interaction with hydroxyl oxygen, similarly, $(ClO_4)^{2-}$ is a nucleophile which seeks an electron deficient atom and makes a possible interaction with hydroxyl hydrogen of the polymer chain resulting in the decrease in the intensity and broadening of the O – H peak in the polymer complexes [29]. The crystallinity of the PVA is altered due to the interaction of the cation/anion of the dopant with the O-H group of PVA which is consistent with the XRD results. The intensity of the medium peak appearing at 1375 cm^{-1} in pure PVA is due to the bending vibration of the O – H group, and is found to decrease with increasing content of $Mg(ClO_4)_2$. The intensity of the sharp band appearing at 2925 cm^{-1} in the pure PVA is attributed to the asymmetric stretching vibration of CH_2 groups, and is found to decrease with an increase in dopant concentration. Further, the peak observed at 1431 cm^{-1} assigned to the C – H bending of pure PVA, is broadened and shifted to lower wavenumbers in the polymer complexes. The peak at 1330 cm^{-1} corresponds to the C – H wagging of pure PVA gets shifted to higher wavenumbers in the polymer complexes. The C – C stretching of pure PVA appearing at 1245 cm^{-1} gets shifted to higher wavenumbers in the polymer complexes. The peak observed at 1089 cm^{-1} in pure PVA is attributed to the C – O stretching. The shifting of this peak to lower

wavenumbers (1089 -1076) in the polymer complexes is an indication of the interaction between the C – O group of PVA and the dopant. The vibration peak appearing at 848 cm^{-1} assigned to C – H rocking mode of PVA is found to be shifted in the polymer complexes. The band appearing at 605 cm^{-1} in pure PVA is assigned to the out of plane O – H bending vibration. It is worth mentioning here that the complexation between the dopant and the residual polyvinyl acetate groups (due to the manufacture of PVA from hydrolysis of Polyvinyl Acetate) is also indicated in the spectra by the presence of peaks at 1733 cm^{-1} and 1245 cm^{-1} resulted from C = O stretching and C – O – C stretching respectively [30,31]. Similar results have been reported in literature for PVA – LiX ($X=ClO_4^-$, $CF_3SO_3^-$, BF_4^-) – DMP gel polymer electrolytes [32]. The asymmetric bending and symmetric stretching of the free anion (ClO_4^{2-}) is indicated by the presence of absorption band at 622 cm^{-1} and 929 cm^{-1} respectively [33,34]. The frequency position and the band shape of the (ClO_4^{2-}) peaks observed at 622 cm^{-1} and 929 cm^{-1} which is considered to be sensitive to anion-cation interaction remains unperturbed with increasing salt concentration in the polymer complexes rules out the possibility of ion association. FTIR analysis strongly suggests the possible coordination sites for the dopant with the polymer as outlined in Fig 3. Peak position shifts and changes in the intensities of various peaks indicate the complexation formed between PVA and $Mg(ClO_4)_2$.

3.3. DSC Studies

The DSC thermograms of pure PVA and its complexes are shown in Fig 4. In the DSC thermogram of pure PVA, a sharp endothermic peak at 223 °C is observed which is assigned to the crystalline melting temperature (T_m) of PVA [24]. After the

incorporation of the $Mg(ClO_4)_2$ in PVA, a significant reduction in the melting temperature is observed for all the polymer electrolytes. This decrease in the T_m and broadening of the melting endotherms can be associated with the interaction between $Mg(ClO_4)_2$ and polymer chains or changes in the alignment of the polymer chains [35]. The area under the curve for the melting endotherm is associated with the crystallinity of the sample. The degree of crystallinity (χ_c) of the same set of samples has been calculated from the computer software using the formula,

$$\chi_c = \frac{H_m}{H_o} \times 100 \qquad (2)$$

where, ΔH_m and ΔH_o are the melting heat of the doped polymer electrolytes and pure PVA (138.6 J/g) respectively. The calculated crystallinity is given in Table. 3. The crystallinity value is found to decrease with the increase in dopant concentration and commensurate with the results obtained by the XRD studies of the polymer electrolyte films.

3.4. Impedance Analysis

The complex impedance plots for different mole ratios of PVA – $Mg(ClO_4)_2$ polymer electrolytes at room temperature (303K) are shown in Fig. 5. The plot shows a high frequency semicircular portion ascribed to the bulk properties of the electrolytes and the low frequency inclined linear region is due to the effect of the blocking electrodes. The high frequency semicircle can be represented as a parallel combination of a resistor and a capacitor, here, the resistor is referred to the migration of ions in the polymer matrix and the capacitor represents the immobile polarised polymer chains in the alternating field.

Also the semicircles are depressed in nature indicating that the ions have different relaxation time. The non-vertical spikes inclined at an angle less than 90° from the real Z′ axis in the low frequency region suggest the surface in-homogeneity at the electrode - electrolyte interface. Due to the effect of the blocking electrodes the mobile ions cannot penetrate the electrode but will form a monolayer close to the surface of each electrode resulting in an electrical double layer [36].

From Fig. 5, it is obvious that as the dopant concentration increases the diameter of the semicircle decreases which is a direct evidence for the decrease in bulk resistance (R_b) value. The disappearance of the high frequency semicircle at higher salt concentrations (20 and 25 mol% $Mg(ClO_4)_2$) indicates the increased charge carrier density and the conductivity is mainly due to ions [36]. The bulk resistance (R_b) of the polymer electrolytes is calculated from the intercept of the high frequency semicircle or low frequency spike on the real impedance (Z') axis. The ionic conductivity (σ) is calculated using the equation $\sigma = t/AR_b$ where t and A are the thickness and the area of the polymer electrolytes respectively. The highest ionic conductivity at room temperature is found to be 8.47×10^{-4} Scm^{-1} for the 20 mol % $Mg(ClO_4)_2$. Hirankumar et al. have found the conductivity of pure PVA to be 2×10^{-10} Scm^{-1} at room temperature [37]. Ulaganathan et al. have studied PVAc based lithium ion conducting polymer electrolytes and obtained conductivity values in the range of 10^{-3} Scm^{-1} [38-40]. The conductivity values of all the polymer electrolytes at room temperature given in Table. 1. It is also found from the table that the conductivity value increases with increasing dopant concentration upto 20 mol% and then decreases. The decrease in conductivity observed

for the sample with 25 mol% of dopant concentration may due to the increase in the degree of crystallinity at higher salt concentration which is in good agreement with the XRD results.

3.5. Temperature Dependant Conductivity

The temperature dependence of electrical conductivity of the polymer films is shown in Fig. 6. The ionic conductivity vs temperature curve shows a linear trend over the entire temperature range studied. The experimental data has been fitted using least squares analysis, a straight line fit (regression > 0.95) has been observed for all the polymer electrolytes. The increase in conductivity with temperature is attributed to two major factors (i) the increased polymer chain mobility due to increased free volume at higher temperature facilitates the ions to hop between adjacent coordination sites and (ii) the equilibrium between dissociated and associated forms of $Mg(ClO_4)_2$ should favour the dissociated ions at higher temperatures [41].

The activation energy (E_a) for the polymer electrolytes has been obtained by the linear fitting of the Arrhenius equation,

$$\sigma = \frac{\sigma_o}{T} \exp \frac{-E_a}{KT} \qquad (3)$$

where σ_o is pre-exponential factor and K is the Boltzmann constant. Table. 1 gives the activation energy (E_a) of all the polymer electrolytes. The decrease in activation energy with increasing dopant concentration can be associated with a decrease in the degree of crystallinity of the host polymer as evidenced from XRD spectra.

3.6. Transference Number Studies

Wagner's polarisation method has been employed to assess the nature of ion transport and to find total ionic transference number (t_{ion}) from current-time plot. In this method, the d.c current is monitored as a function of time on the application of a small d.c voltage of (0.7 V) across the SS/SPE/SS. Fig. 7 shows the current vs time plot for the polymer electrolyte with highest conductivity (80 PVA : 20 $Mg(ClO_4)_2$) . It is observed from the plot, the sudden drop of current within first 10 minutes time hints that more contribution for conductivity is due to ions than electrons. The value of t_{ion} was evaluated using the following equation,

$$t_{ion} = \frac{i_T - i_e}{i_T} \qquad (4)$$

where, i_T is the total current and i_e is the residual current. The total transport numbers calculated for the polymer electrolytes have been listed in Table. 3. The t_{ion} value was found to be close to unity, which leads one to conclude that the charge carriers are ions. The diffusion coefficients and mobility of cations and anions of each polymer electrolytes have been calculated from the measured values of conductivity and cation transference number, t_+, using the following formulas [42],

$$D_+ + D_- = \left(\frac{KT}{ne^2}\right) \qquad (5)$$

$$t_+ = \frac{D_+}{D_+ + D_-} \qquad (6)$$

$$\mu_{tot} = \mu_+ + \mu_- = \frac{\sigma}{ne} \qquad (7)$$

$$t_+ = \frac{\mu_+}{\mu_+ + \mu_-} \qquad (8)$$

Where,

'e' charge of the electron;

'μ_+' ionic mobility of cation;

'μ_-' ionic mobility of anion;

'k' Boltzmann constant;

'D_+' diffusion coefficient of cation;

'D_-' The diffusion coefficient of anion;

'T' Absolute temperature;

n = N x ρ x molar ratio of salt / molecular weight of the salt

'n' number of molecules cm^{-3}

'N' Avogadro number

'ρ ' density of the salt

From the values given in Table: 3, one can conclude that the cation mobility μ_+ has greater value than the ionic mobility of anions μ_-. The same behaviour also can be detected for D_+. Hence, the study of transference number measurements leads to the conclusion that the conductivity has been influenced by the μ_+ and D_+. The above result supports the conductivity values obtained for the polymer electrolytes.

3.7. Frequency Dependent Conductivity Analysis

The frequency dependent conductivity is a prominent method to relate the macroscopic measurement to the microscopic movement of the ions. The ac conductivity as a function of angular frequency for all the polymer electrolytes at room temperature is shown in Fig. 8. The plot consists of two regions within the measured frequency range, i) a low

frequency dispersion region, and (ii) a frequency independent plateau region. The ac conductivity $\sigma(\omega)$ obeys the Joncher's power law and it is found to vary with angular frequency ω.

$$\sigma(\omega) = \sigma_{dc} + A\omega^{n} \qquad (9)$$

where σ_{dc} is the dc conductivity and A and n are temperature dependent parameters. At low frequencies the charge carriers accumulate at the electrode- electrolyte interface, reducing the number of mobile ions responsible for conductivity. As the frequency increases the space charge build up at the electrode electrolyte interface is minimized and the mobile ions contribute to high value of conductivity [43,44]. It is observed that the ac conductivity increases with increase in dopant concentration indicating the increase in the available charge carriers and polymer segmental mobility.

3.8. Dielectric Analysis

The dielectric permittivity (ε') versus log ω for different compositions of PVA – $Mg(ClO_4)_2$ polymer electrolytes at room temperature are given in Fig. 9. A high value of dielectric permittivity is observed at low frequencies due to the accumulation of charge carriers at the electrode – electrolyte interface representing the non – Debye type of behaviour [45] in the polymer electrolytes. At high frequencies the polarity reversal of the field is very quick leading to inhibition of the polarisation of the dipoles along the field direction resulting in less ion diffusion towards the field direction. This leads to the low value of dielectric permittivity value at high frequencies [46]. A high positive

dielectric permittivity is obtained for the polymer electrolyte system with 20 mol% $Mg(ClO_4)_2$ indicating the increase in the charge carrier density.

3.9. Frequency Dependent Loss Tangent

The relaxation process of charge carriers in polymer electrolytes can be understood by plotting tan δ as a function of angular frequency. From the plot (Fig. 10) it is evident that the tan δ value increases with increasing frequency, reaches a maximum and then decreases. As the salt concentration increases, the frequency at which the peak maximum occurs gets shifted to higher frequency side and also there appears a low frequency dispersion region which is due to interfacial polarisation [45]. The height of the peak also decreases as there is an increase in the dopant concentration indicating a decrease in the relaxation time. This high frequency relaxation is called as the β-relaxation which may be due to the movement of the hydroxyl groups of the host polymer called dipolar group relaxation [47]. The appearance of a new low frequency peak at higher salt concentration may be due to the movement of the main chain of the polymer called the α - relaxation [48] The increase in the dopant concentration increases the amorphous nature of the polymer electrolytes which creates more number of hopping sites for the mobile ions in the polymer electrolyte. In amorphous region the polymer chains are irregular, more flexible and entangled and the dipoles in the side chain of the polymer are more flexible and will be able to orient themselves easily and rapidly with respect to the alternating field. Thus, the fast segmental motion coupled with the mobile ions enhances the ion transport properties of the polymer electrolytes which is in good agreement with the DSC

and XRD results. The relaxation parameters were calculated for all the samples at room temperature and listed in Table. 1 using the following relations,

$$\omega \tau = 1 \quad (10)$$

$$\omega = 2\pi f_{max} \quad (11)$$

$$\tau = \frac{1}{\omega} \quad (12)$$

Where τ and ω are the relaxation time of the hopping process and angular frequency of the external field respectively. The decrease in relaxation time with increasing salt concentration is a direct evidence for the enhanced conductivity.

3.10. Linear Sweep Voltammetry

The electrochemical stability of the highest conducting sample (80 mol% PVA: 20 mol% $Mg(ClO_4)_2$) was determined by linear sweep voltammetry recorded on SS/SPE/Mg cell at a scan rate of 1 mVS^{-1}. Fig. 11 displays the current –voltage response obtained by applying voltage to the cell. The potential limit for the electrolyte system was swept from 0V towards positive values until a large current is obtained. The sudden rise in current observed from the plot is attributed to the electrolyte decomposition at the blocking electrode interface [49]. It found that the SPE is stable upto 2 V. Asmara et al. reported similar results (~2.4 V) for PMMA based gel polymer electrolytes [18].

3.11. Cyclic Voltammetry

The cyclic voltammogram for the cells containing electrolyte sample 80 mol% PVA : 20 mol% $Mg(ClO_4)_2$ sandwiched between two symmetrical magnesium electrodes are shown in Fig. 12. The CV of the cell with SS electrodes are also shown for comparison. In the case of SS cell assembly, no current peaks were observed and it can be inferred that, the electrodeposition of Mg is not facilitated on the SS electrode. However, cathodic and anodic current peaks are observed for the cells with Mg electrodes, corresponding to the reaction,

$$Mg^{2+} + 2e \Leftrightarrow Mg \qquad (13)$$

which serves as an evidence for the reversibility of the Mg/Mg^{2+} reaction in the solid polymer electrolyte media. The value of peak potential separation is much greater than 0.03 V, similar to the case of Li/SPE/Li cells [50]. This is because of the polarisation of the symmetrical electrodes (Mg/SPE/Mg) during the voltage sweep and also Mg surface is covered with a passivating layer. Similar reports have been reported by Girish Kumar et. al. and Pandey et.al for magnesium based gel polymer electrolytes [51,7]. The charges associated with the current peaks imply that the anodic charge is only 90 % of the cathodic charge, suggesting the quasi reversible nature of the Mg electrode.

4. CONCLUSION

The polymer electrolytes containing Mg^{2+} as the conducting species have been prepared by solution casting method and evaluated using ac impedance, FTIR, XRD, DSC and CV. The prepared SPEs showed a steady increase in conductivity with increasing salt composition and a maximum conductivity of 10^{-4} S/cm (8.47×10^{-4} S/cm) was observed at room temperature for the polymer electrolyte with 80 mol% PVA: 20

mol% $Mg(ClO_4)_2$. The change in intensity, shape and position of the FTIR peaks confirms the complexation. The amorphous nature of the polymer matrix has been confirmed by XRD. The reduction in the melting endothermic peak towards lower temperature confirms the increase in amorphicity of the polymer electrolytes with increasing salt concentration. The cyclic voltammetry suggests the existence of electrochemical equilibrium between the Mg metal and the Mg^{2+} ions in the polymer electrolyte. Several studies related to Mg/SPE interface are under progress.

ACKNOWLEDGEMENT

One of the authors Mrs. Mangalam. R would like to thank the Principal and Management, PSG Institute of Technology and Applied Research for the support extended towards this research work.

REFERENCES

1. Rathika, R.; Austin Suthanthiraraj, S. Ionic Interactions and Dielectric Relaxation of PEO/PVDF-Mg[$(CF_3SO_2)_2N_2$)] Blend Electrolytes for Magnesium Ion Rechargeable Batteries. Macromol. Res. **2016**, *24*, 422-428.
2. Zheng, Y.P.; NuLi, Y.N.; Chen, Q.; Wang, Y.; Yang, J.; Wang, J.L. Magnesium cobalt silicate materials for reversible magnesium ion storage. Electrochim. Acta. **2012**, *66*, 75-81.
3. Pour, N.; Gofer, Y.; Major, D.T.; Aurbach, D. Structural analysis of electrolyte solutions for rechargeable Mg batteries by stereoscopic means and DFT calculations. J. Am. Chem. Soc. **2011**, *133*, 6270-6278.

4. Se-Young Ha; Yong-Won Lee; Sang Won Woo; Bonjae Koo; Jeom-Soo Kim; Jaephil Cho; Kyu Tae Lee Nam-Soon Choi**.** Magnesium(II) Bis(trifluoromethane sulfonyl) Imide-Based Electrolytes with Wide Electrochemical Windows for Rechargeable Magnesium Batteries. ACS Appl. Mater. Interfaces. **2014**, *6*, 4063 -4073.

5. Pandey, G.P.; Agrawal, R.C.; Hashmi, S.A. Performance studies on composite gel polymer electrolytes for rechargeable magnesium battery application. J. Phys. Chem. Solids. **2011**, *72*, 1408-1413.

6. Nobuko Yoshimoto; Yoichi Tomonaga; Masashi Ishikawa; Masayuki Morita. Ionic conductance of polymeric electrolytes consisting of magnesium salts dissolved in cross-linked polymer matrix with linear polyether. Electrochim Acta 2001, *46*, 1195–1200.

7. Pandey, G.P.; Hashmi, S.A. Experimental investigations of an ionic liquid based, magnesium ion conducting polymer gel electrolyte. J. Power Sources **2009**, *187*, 1745-1751.

8. Xin Tang; Ravi Muchakayala; Shenhua Song; Zhongyi Zhang; Anji Reddy Polu. A study of structural, electrical and electrochemical properties of PVdF-HFP gel polymer electrolyte films for magnesium ion battery applications J Ind Eng Chem. **2016**, *37*, 67-74.

9. Eslam M.Sheha; Mona M. Nasr; Mabrouk K. El-Mansy. The role of $MgBr_2$ to enhance the ionic conductivity of PVA/PEDOT:PSS polymer composite. Journal of Advanced Research **2015,** *6*, 563-569.

10. Nobuko Yoshimoto;Shin Yakushiji; Masashi Ishikawa; Masayuki Morita. Rechargeable magnesium batteries with polymeric gel electrolytes containing magnesium salts. Electrochim. Acta. **2003** , *48*, 2317-2322.

11. Girish Kumar, G.; Munichandraiah, N. Effect of plasticizers on magnesium-poly(ethyleneoxide) polymer electrolyte. J Electroanal Chem. **2000,** *49*, 42-50.

12. Yuyan Shao; Nav Nidhi Rajput; Jianzhi Hu; Mary Hu, Tianbiao Liu; Zhehao Wei; Meng Gu; Xuchu Deng; Suochang Xu; Kee Sung Han; Jiulin Wang; Zimin Nie; Guosheng Li; Kevin R. Zavadil; Jie Xiao; Chongmin Wang; Wesley A. Henderson; Ji-Guang Zhang; Yong Wang; Karl T. Mueller; Kristin Persson; Jun Liu. Nanocomposite polymer electrolyte for rechargeable magnesium batteries. N Energy **2015,** *12*, 750-759.

13. Jyoti Sharma; Hashmi, S. A. Magnesium ion transport in poly(ethylene oxide)-based polymer electrolyte containing plastic-crystalline succinonitrile. J of Solid State Electrochem. **2013**, *17*, 2283-2291.

14. Yogesh Kumar; Hashmi, S.A.; Pandey, G.P. Ionic liquid mediated magnesium ion conduction in poly(ethylene oxide) based polymer electrolyte. Electrochim. Acta. **2011,** *56*, 3864-3873.

15. Zainol, N. H.; Samin, S.M.; Othman, L.; Md Isa, K.B.; Chong W.G.; Osman Z. Magnesium Ion-Based Gel Polymer Electrolytes: Ionic Conduction and Infrared Spectroscopy Studies. Int. J. Electrochem. Sci. **2013**, *8*, 3602-3614.

16. Osman, Z.; Zainol, N.H.; Samin, S.M.; Chong, W.G.; Md Isa, K.B.; Othman, L.; Supa'at I.; Sonsudin, F. Electrochemical Impedance Spectroscopy Studies of Magnesium-Based Polymethylmethacrylate Gel Polymer Electroytes. Electrochim. Acta. **2014,** *131*, 148-153.

17. Tripathi, S. K.; Amrita Jain; Ashish Gupta; Manju Mishra. Electrochemical studies on nanocomposite polymer electrolyte. J Solid State Electrochemistry **2012,** *16*, 1799-1806.

18. Asmara, S. N.; Kufian, M . Z.; Majid, S. R.; Arof, A.K. Preparation and characterization of magnesium ion gel polymer electrolytes for application in electrical double layer capacitors. Electrochim. Acta. **2011**, *57*, 91-97.

19. Choudhury, N. A.; Sampth, H.; Shukla, A. K. Hydrogel – Polymer for electrochemical capacitors: an overview. Energy Environ. Sci. **2009**, *2*, 55-67.

20. Choudhary, N.A.; Shukla, A.K.; Sampath, S.; Pitchumani, S. Cross-Linked Polymer Hydrogel Electrolytes for Electrochemical Capacitors. J. Electrochem. Soc. **2006,** *153*, A614-620.

21. Mohamad, A.A.; Arof, A.K. Plasticized alkaline solid polymer electrolyte system. Mater. Lett. **2007**, *61*, 3096-3099.

22. Polu, A. R.; Kumar, R. Ionic Conductivity and Discharge Characteristic Studies of PVA-Mg $(CH_3COO)_2$ Solid Polymer Electrolytes. Int. J Polymer. Mater. **2013**, *62*, 76-80.

23. Polu, A. R.; Kumar, R. Preparation and characterization of pva based solid polymer electrolytes for electrochemical cell applications. Chin. J. Polym. Sci. **2013**, *31* , 641-648.

24. Pundir, S.S; Kuldeep Mishra; Rai, D.K. Poly(vinyl)alcohol/1-butyl-3-methylimidazolium hydrogen sulfate solid polymer electrolyte: Structural and electrical studies. Solid State Ionics **2015**, *275*, 86-91

25. Jaipal Reddy, M; Chu, P.P. Effect of Mg^{2+} on PEO morphology and conductivity. Solid State Ionics **2002**, *149*, 115-123.

26. Hodge, R. M.; Edward, G. H; Simon, G. P. Water absorption and states of water in semicrystalline poly(vinyl alcohol) films. Polymer **1996**, *37*, 1371-1376.

27. Arbi Fattoum; Mourad Arous; Rolando Pedicini; Alessandra Carbone; Clarence Charnay. Conductivity and dielectric relaxation in crosslinked PVA by oxalic and citric acids. Polymer Science Ser. A. 2015, *57*, 321-329.

28. Pandey, G.P.; Agrawal, R.C.; Hashmi, S.A. Magnesium ion-conducting gel polymer electrolytes dispersed with fumed silica for rechargeable magnesium battery application. J. Solid State Electrochem. **2011**, *15*, 2253-2264.

29. Hsien-Wei Chen, HongYao Xu, Chih-Feng Huang, Feng-Chih Chang, Novel Polymer Electrolyte Composed of Poly(ethylene oxide), Lithium Triflate, and Benzimidazole, J. Applied Polymer Science **2004**, *91*, 719-725.

30. Shehap, A.M. Thermal and spectroscopic studies of polyvinyl alcohol /sodium carboxy methyl cellulose blends. Egypt J Solid **2008**, *31*, 75-91.

31. Krimm, S.; Liang, C.Y.; Sutherland, G.B.B.M. Infrared spectra of high polymers. Polyvinyl alcohol. J. Polym. Sci., Part A: Polym. Chem. **1956**, *22*, 227-247.

32. Rajendran, S.; Sivakumar, M.; Subadevi, R. Li-ion conduction of plasticized PVA solid polymer electrolytes complexed with various lithium salts. Solid State Ionics **2004**, *167*, 335-339.

33. Aruna, S.; Anuradha, A.; Thomas, P.C; Gulam Mohammed, M.; Rajasekar, S.A.; Vimalan, M.; Mani, G.; Sagayaraj, P. Growth, optical and thermal studies of L-arginine perchlorate—A promising non-linear optical single crystal. Indian J. Pure Appl. Phys. **2007**, *45* 524-528.

34. Miller, F.A.; Carlson, G.C.; Bentley, F.F.; Jones, W.H. Infra-red spectra of inorganic ions in the cesium bromide region (700-300 cm^{-1}). Spectrochim. Acta. **1960,** *16*, 135-235.

35. Prajapati, G.K.; Roshan, R.; Gupta, P.N. Effect of plasticizer on ionic transport and dielectric properties of PVA–H_3PO_4 proton conducting polymeric electrolytes. J. Phys. Chem. Solids **2010**, *71*, 1717-1723.

36. Macdonald, J.R. Impedance Spectroscopy Emphasizing Solid Materials and System, John Wiley & sons, NewYork,. **1987**.

37. Hirankumar, G.; Selvasekarapandian, S.; Kuwata, N.; Kawamura, J.; Hattori, T. Thermal, electrical and optical studies on the poly(vinyl alcohol) based polymer electrolytes. J. Power Sources **2004**, *144*, 262-267.

38. Ulaganathan, M; Rajendran, S. Li ion conduction on plasticizer-added PVAc-based hybrid polymer electrolytes. Ionics **2010**, *16*, 667-672.

39. Ulaganathan, M; Rajendran, S. Novel Li ion conduction on polyIvinyl acetate)-based hybrid polymer electrolytes with double plasticizers. J Appl Electrochem **2011**, *41*, 83-88.

40. Ulaganathan, M; Rajendran, S. Effect of different salts on PVAc/PVdF-co-HFP based polymer blend electrolytes. J. Applied Polymer Science **2010**, *118*, 646-651.

41. Druger, S.D.; Nitzan A.; Ratner, M.A. Applications of dynamic bond percolation theory to the dielectric response of polymer electrolytes. J. Chem. Phys. **1983**, *79*, 3133-.

42. Sikkanthar, S.; Karthikeyan, S.; Selvasekarapandian, S.; Vinoth Pandi, D.; Nithya, S.; Sanjeeviraja, C. Electrical conductivity characterization of polyacrylonitrile-ammonium bromide polymer electrolyte system. J Solid State Electrochem **2015**, 19, 987-999.

43. Federico Bertasi; Keti Vezzu; Guinevere A. Giffin; Tetiana Nosach; Paul Sideris; Steve Greenbaum; Michele Vittadello; Vito Di Noto. Single-ion-conducting

nanocomposite polymer electrolytes based on PEG400 and anionic nanoparticles: Part 2. Electrical characterization. Int. J. Hydrogen Energy. **2014**, *39*, 2884-2895.

44. Namrata Tripathi; Awalendra K. Thakur; Archana Shukla; David T. Marx. Ion transport study in polymer-nanocomposite films by dielectric spectroscopy and conductivity scaling. Physica B **2015**, *468*, 50-56.

45. Ramesh, S.; Arof, A.K. Ionic conductivity studies of plasticized poly(vinyl chloride) polymer electrolytes. Mater. Sci. Eng., B. **2001,** *85*, 11-15.

46. Woo, H.J.; Majid, S.R.; Arof, A.K. Dielectric properties and morphology of polymer electrolyte based on poly (ε -caprolactone) and ammonium thiocyanate. Mater. Chem. Phys. **2012,** *134*, 755-761.

47. Tareev, B. **1979**. Physics of Dielectric materials, MIR Publishers, Moscow.

Tager, A.**1978,** Physical chemistry of polymers. MIR Publishers, Moscow.

Nurul Husna Zainol; Mohd Zharfan Mohd. Halizan; Woon Gie Chong; Zurina Osman. Ionic Transport and Electrochemical properties of PMMA based gel polymer electrolytes for magnesium batteries. ADV MAT RES **2014**, *1024*, 348-351.

48. Munichandraiah, N.; Scanlon, L.G.; Marsh, R.A.; Kumar, B.; Sicar, A.K. Influence of zeolite on electrochemical and physicochemical properties of poly(ethyleneoxide) solid electrolyte. J. Appl. Electrochem. **1995**, *25*, 857-863.

49. Girish Kumar, G.; Munichandraiah, N. Polymethylmethacrylate – magnesium triflate gel polymer electrolyte for solid state magnesium battery application. Electrochim. Acta **2002**, *47*,1013-1022.

Table 1. Composition, crystallite size, ac conductivity, hopping frequency and relaxation time values of the solid polymer electrolytes.

Sample Code	Composition	Crystallite size, A°	ac conductivity S/cm (303 K)	Hopping frequency ω_p (hz)	Relaxation time τ (s)	Activation energy (E_a)	Regression value
Pure PVA	100% PVA	0.19					
95:5	95mol%PVA + 5mol%$Mg(ClO_4)_2$	-	3.2×10^{-9}	8.16×10^{2}	1.22×10^{-3}	0.67	0.95
90:10	90mol%PVA + 10mol%$Mg(ClO_4)_2$	-	2.8×10^{-6}	2.66×10^{5}	3.67×10^{-6}	0.59	0.99
85:15	85mol%PVA + 15mol%$Mg(ClO_4)_2$	0.11	2.1×10^{-5}	6.28×10^{6}	1.59×10^{-7}	0.46	0.95
80:20	80mol%PVA + 20mol%$Mg(ClO_4)_2$	0.02	0.84×10^{-3}	1.31×10^{7}	7.58×10^{-8}	0.38	0.99
75:25	75mol%PVA + 25mol%Mg(Cl	0.10	0.26×10^{-3}	3.14×10^{6}	3.18×10^{-7}	0.39	0.97

	$O_4)_2$						

Table 2. FT-IR absorption bands and their assignments for pure PVA and the polymer complexes.

Pure PVA	**95:5**	**90:10**	**85:15**	**80:20**	**75:25**	**Band Assignments**
3307	3340	3342	3379	3392	3373	OH stretching
2925	2925	2929	2929	2925	2923	CH_2 asymmetric stretching
1733	1716	1710	1708	1699	1695	C=O stretching
1431	1429	-	1434	1429	1429	CH_2 bending
1375	1379	1380	1382	1379	1379	O – H Bending
1245	1263	1272	1278	1276	1276	C- O-C stretching
1089	1083	1082	1068	1076	1076	C-O stretching
848	852	844	844	850	840	C – H rocking
605	-	-	-	-	-	out of plane OH bending
-	621	622	622	622	621	ClO_4^- asymmetric bending
-	946	929	929	929	929	ClO_4^- symmetric stretching

Table 3. Ionic mobility, diffusion coefficient of cations & anions, melting temperature and degree of crystallinity values for some selected SPE.

Sample	t_{ion}	N (cm^{-3})	D_+ ($cm\ s^{-1}$)	D_- ($cm\ s^{-1}$)	μ_+ ($cm^2\ V^{-1}\ S^{-1}$)	μ_- ($cm^2\ V^{-1}\ S^{-1}$)	T_m ^oC	χ_c
Pure PVA	-	-	-	-	-	-	223	38
85:15	0.92	$4.8 x10^{22}$	$6.5x10^{-11}$	$5.7x10^{-12}$	$2.5x10^{-8}$	$0.21x10^{-8}$	190	15
80:20	0.94	$6.4x10^{22}$	$1.9x10^{-9}$	$1.2x10^{-10}$	$7.7x10^{-8}$	$4.9x10^{-9}$	131	8
75:25	0.93	$8.0x10^{22}$	$4.9x10^{-10}$	$3.6x10^{-11}$	$1.8x10^{-8}$	$1.4x10^{-9}$	132	11

Fig. 1. XRD pattern of a) $Mg(ClO_4)_2$, b) Pure PVA, c) 85 mol % PVA : 15 mol % $Mg(ClO_4)_2$, d) 80 mol % PVA : 20 mol % $Mg(ClO_4)_2$, e) 75 mol % PVA : 25 mol % $Mg(ClO_4)_2$

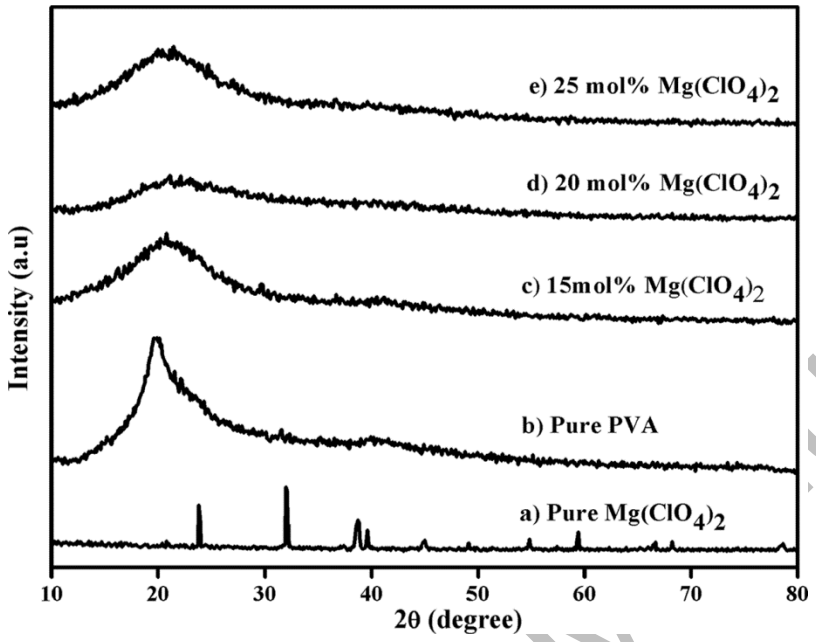

Fig. 2. FTIR pattern of a) Pure PVA b) 95 mol % PVA : 5 mol % $(ClO_4)_2$, c) 90 mol % PVA : 10 mol % $Mg(ClO_4)_2$, d) 85 mol % PVA : 15 mol % $Mg(ClO_4)_2$, e) 80 mol % PVA : 20 mol % $Mg(ClO_4)_2$, f) 75 mol % PVA : 25 mol % $Mg(ClO_4)_2$.

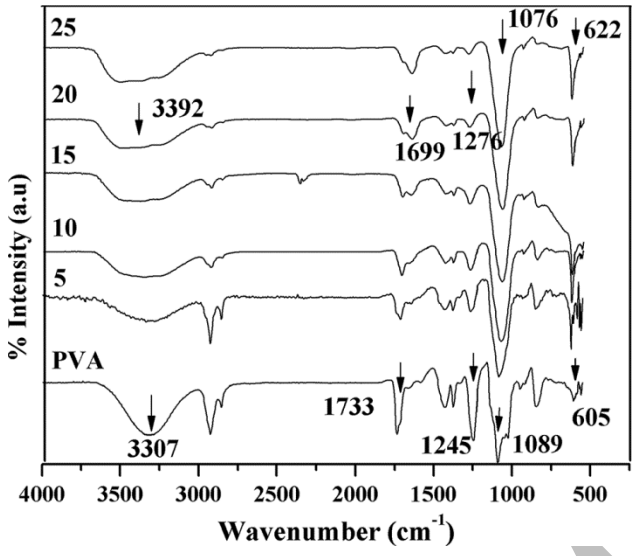

Fig. 3. Possible interaction of the mechanism of the dopant with the polymer host

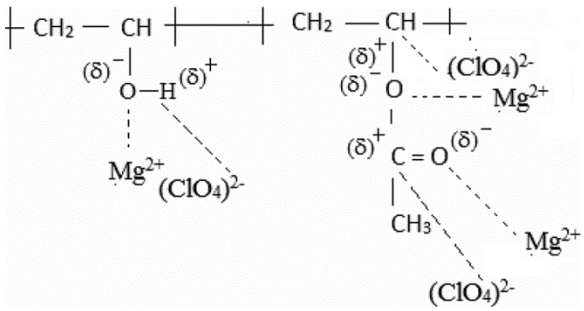

Fig. 4. DSC thermograms of a) Pure PVA, b) 85 mol % PVA : 15 mol % $Mg(ClO_4)_2$, c) 80 mol % PVA : 20 mol % $Mg(ClO_4)_2$, d) 75 mol % PVA : 25 mol % $Mg(ClO_4)_2$

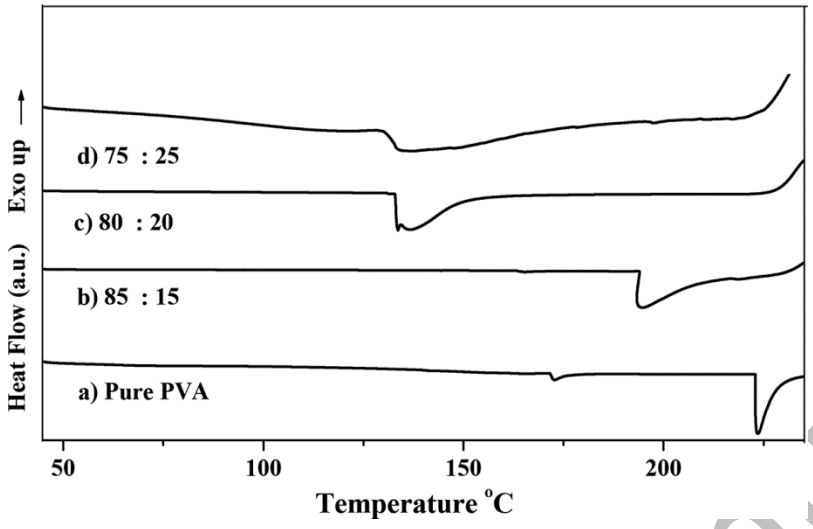

Fig. 5. Complex impedance plots of a) 95 mol % PVA : 5 mol % $Mg(ClO_4)_2$, b) 90 mol % PVA : 10 mol % $Mg(ClO_4)_2$, c) 85 mol % PVA : 15 mol % $Mg(ClO_4)_2$, d) 80 mol % PVA : 20 mol % $Mg(ClO_4)_2$, e) 75 mol % PVA : 25 mol % $Mg(ClO_4)_2$ at RT.

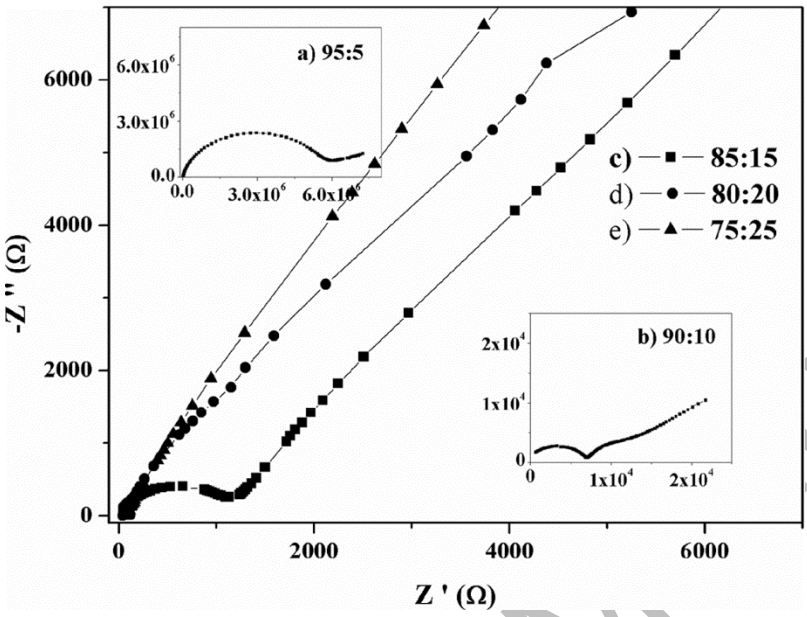

Fig.6 . Log σ vs 1000/T plot of a) 95 mol % PVA : 5 mol % $Mg(ClO_4)_2$, b) 90 mol % PVA : 10 mol % $Mg(ClO_4)_2$, c) 85 mol % PVA : 15 mol % $Mg(ClO_4)_2$, d) 80 mol % PVA : 20 mol % $Mg(ClO_4)_2$, e) 75 mol % PVA : 25 mol % $Mg(ClO_4)_2$.

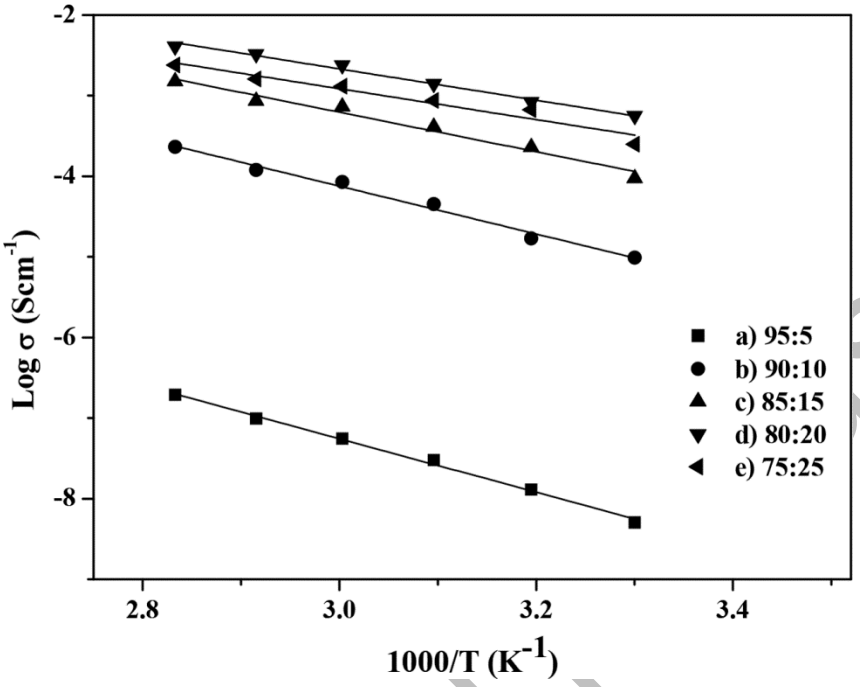

Fig. 7. Current vs time curve for 80 PVA : 20 $Mg(ClO_4)_2$ polymer electrolyte

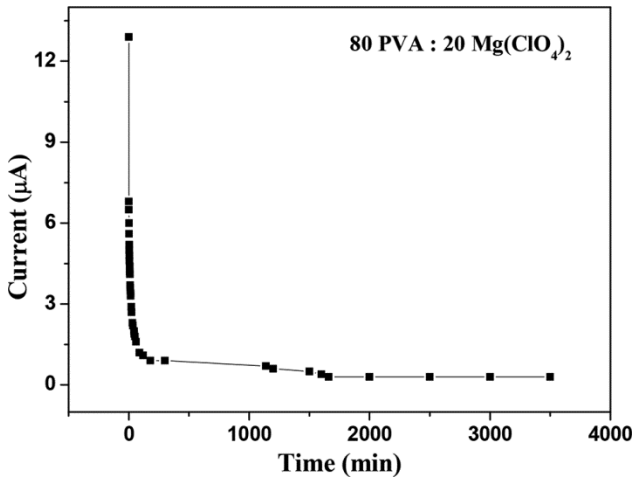

Fig. 8. ac conductivity plots of a) 90 mol % PVA : 10 mol % $Mg(ClO_4)_2$, b) 85 mol % PVA : 15 mol % $Mg(ClO_4)_2$, c) 80 mol % PVA : 20 mol % $Mg(ClO_4)_2$, d) 75 mol % PVA : 25 mol % $Mg(ClO_4)_2$ at RT

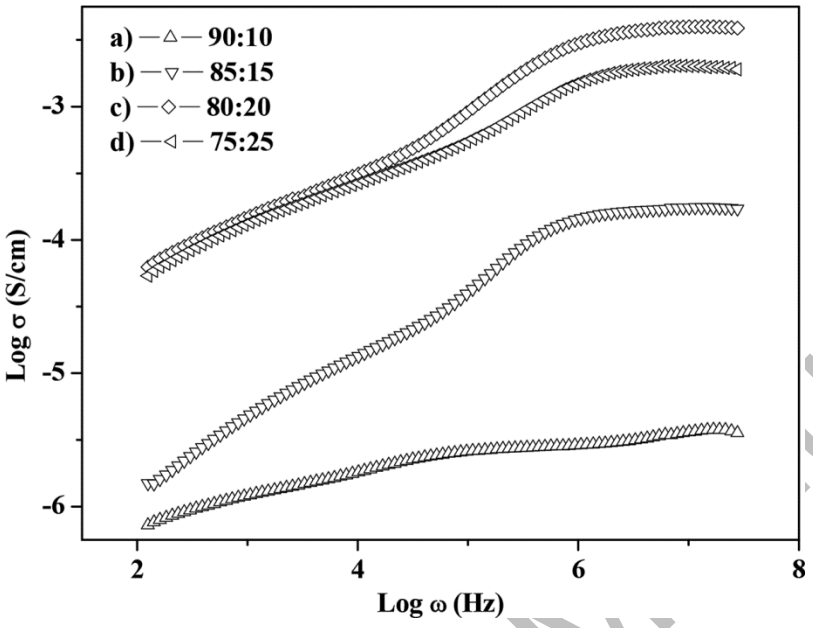

Fig. 9. Dielectric permittivity spectra of a) 95 mol % PVA : 5 mol % $Mg(ClO_4)_2$, b) 90 mol % PVA : 10 mol % $Mg(ClO_4)_2$, c) 85 mol % PVA : 15 mol % $Mg(ClO_4)_2$, d) 80 mol % PVA : 20 mol % $Mg(ClO_4)_2$, e) 75 mol % PVA : 25 mol % $Mg(ClO_4)_2$ at RT

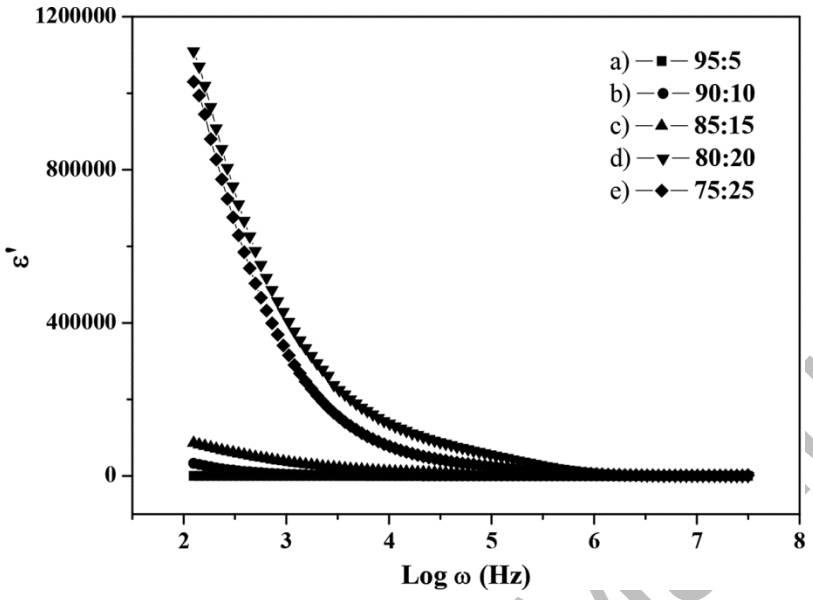

Fig 10. Frequency dependent loss tangent spectra of a) 95 mol % PVA : 5 mol % $Mg(ClO_4)_2$, b) 90 mol % PVA : 10 mol % $Mg(ClO_4)_2$, c) 85 mol % PVA : 15 mol % $Mg(ClO_4)_2$, d) 80 mol % PVA : 20 mol % $Mg(ClO_4)_2$, e) 75 mol % PVA : 25 mol % $Mg(ClO_4)_2$ at RT

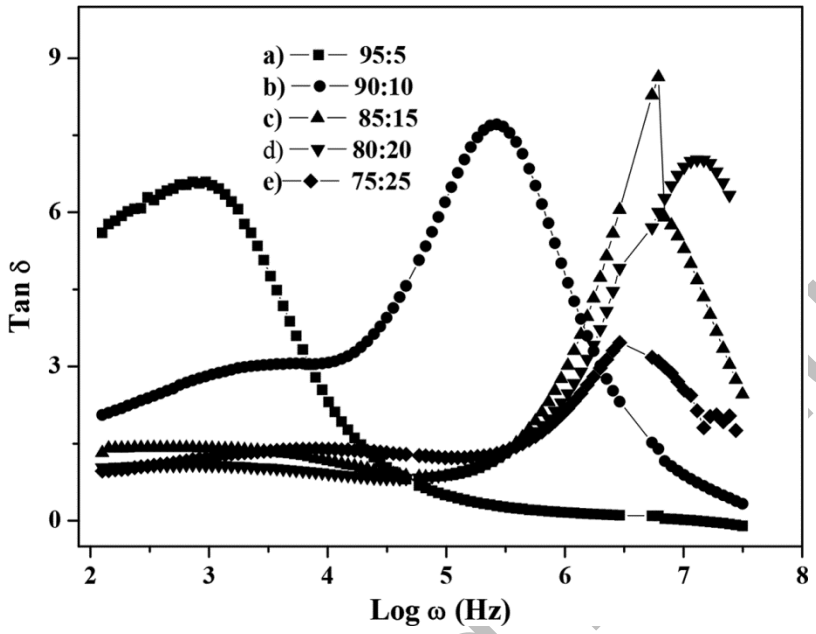

Fig. 11. LSV of cell SS/SPE/Mg recorded at room temperature at a scan rate of $1mVs^{-1}$.

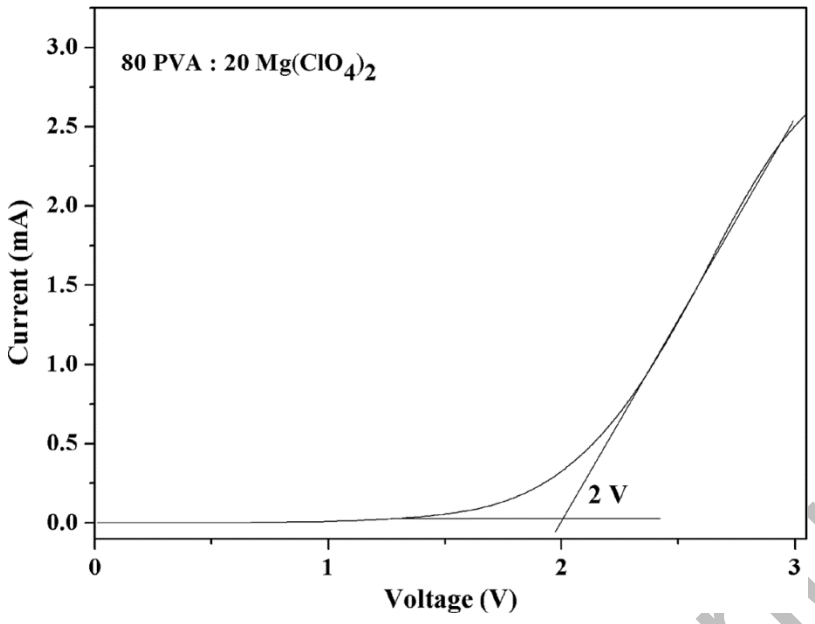

Fig. 12. Cyclic voltammogram of cells: SS/SPE/SS and Mg/SPE/Mg recorded at room temperature at a scan rate of $5mVs^{-1}$.